Cancer Research

Mesenchymal Stem Cells Promote Hepatocarcinogenesis via lncRNA–MUF Interaction with ANXA2 and miR-34a

Xinlong Yan[1,2], Dongdong Zhang[3,4], Wei Wu[3,4,5], Shuheng Wu[3,4,5], Jingfeng Qian[3,4], Yajing Hao[3,4,5], Fang Yan[6], Pingping Zhu[2], Jiayi Wu[2,5], Guanling Huang[2], Yinghui Huang[1], Jianjun Luo[3,4], Xinhui Liu[1], Benyu Liu[2,5], Xiaomin Chen[3,4], Ying Du[2], Runsheng Chen[3,4,5], and Zusen Fan[2,5]

Abstract

Accumulating evidence suggests that cancer-associated mesenchymal stem cells (MSC) contribute to the development and metastasis of hepatocellular carcinoma (HCC). Aberrant expression of long noncoding RNAs (lncRNA) has been associated with these processes but cellular mechanisms are obscure. In this study, we report that HCC-associated mesenchymal stem cells (HCC-MSC) promote epithelial–mesenchymal transition (EMT) and liver tumorigenesis. We identified a novel lncRNA that we termed *lncRNA–MUF* (MSC-upregulated factor) that is highly expressed in HCC tissues and correlated with poor prognosis. Depleting *lncRNA–MUF* in HCC cells repressed EMT and inhibited their tumorigenic potential. Conversely, lncRNA–MUF overexpression accelerated EMT and malignant capacity. Mechanistic investigations showed that *lncRNA–MUF* bound Annexin A2 (ANXA2) and activated Wnt/β-catenin signaling and EMT. Furthermore, lncRNA-MUF acted as a competing endogenous RNA for miR-34a, leading to Snail1 upregulation and EMT activation. Collectively, our findings establish a lncRNA-mediated process in MSC that facilitates hepatocarcinogenesis, with potential implications for therapeutic targeting. *Cancer Res; 77(23); 6704–16. ©2017 AACR.*

Introduction

Hepatocellular carcinoma (HCC) is the fifth most common cancer and the third leading cause of cancer-related mortality worldwide (1). HCC has been previously thought as a largely cell-autonomous process involving genetically transformed hepatic parenchymal cells or progenitor cells caused by hepatitis B virus/hepatitis C virus infection, food contamination, and nonalcoholic fatty liver disease (2). Recently, interactions between the tumor microenvironment and HCC cells have been increasingly appreciated as pivotal contributors to tumorigenesis and metastasis (3–5). Mesenchymal stem cells (MSC), first identified in the bone marrow, are a heterogeneous group of progenitor cells for tissue maintenance in physiologic conditions. MSCs have been increasingly appreciated as important parts of the tumor microenvironment in the last 10 years, and they can be recruited from the bone marrow or peripheral blood to participate in stromal desmoplastic reactions at tumor sites (4, 6). However, the number of MSCs in the peripheral blood is very low, even in mobilized peripheral blood (7), thus, these recruited MSCs cannot likely to be the main source of MSCs in the tumor microenvironment.

Recently, da Silva and colleagues (8) hypothesized that mouse MSCs reside in the perivascular zone. In addition, Crisan and colleagues (9) further identified human MSCs in the perivascular regions of multiple human organs. On the basis of these findings as well as the high vascular density and strong desmoplastic reaction in HCC tissues, we speculated that there may be numerous of MSCs localized in the perivascular region of HCC sites. Thereafter, we have provided the first evidence that HCC-associated MSCs (HCC-MSC) exist in primary HCC tissues (3). A thorough investigation of the interaction between MSCs and HCC cells might strengthen our understanding of the tumor microenvironment in HCC pathogenesis.

Recently, whole transcriptome sequencing has identified a large number of long noncoding RNAs (lncRNA), larger than 200 nucleotides and lack coding potential (10). Increasing evidence has indicated that lncRNAs can participate in many physiologic or pathologic processes through diverse mechanisms including RNA–protein (11–14) or RNA–RNA interactions (15). Dysregulated lncRNAs have been reported to regulate HCC proliferation (16), metastasis (17), and recurrence (18). However, the role of lncRNAs in MSC-mediated hepatocarcinogenesis remains unknown.

[1]College of Life Science and Bioengineering, Beijing University of Technology, Beijing, China. [2]Key Laboratory of Infection and Immunity, Institute of Biophysics, Chinese Academy of Sciences, Beijing, China. [3]Key Laboratory of RNA Biology, Institute of Biophysics, Chinese Academy of Sciences, Beijing, China. [4]Beijing Key Laboratory of Noncoding RNA, Institute of Biophysics, Chinese Academy of Sciences, Beijing, China. [5]University of Chinese Academy of Sciences, Beijing, China. [6]Department of Tissue Engineering, Beijing Institute of Transfusion Medicine, Beijing, China.

Note: Supplementary data for this article are available at Cancer Research Online (http://cancerres.aacrjournals.org/).

X. Yan and D. Zhang contributed equally to this article.

Corresponding Authors: Xinlong Yan, Beijing University of Technology, No. 100 Pingleyuan, Chaoyang District, Beijing 100124, China. Phone: 8610-6693-1949; Fax: 8610-6816-7357; E-mail: yxlong2000@bjut.edu.cn; Runsheng Chen, Institute of Biophysics, Chinese Academy of Sciences, Beijing 100101, China. E-mail: rschen@sun5.ibp.ac.cn; and Zusen Fan, fanz@moon.ibp.ac.cn

doi: 10.1158/0008-5472.CAN-17-1915

In this study, we investigated the contribution of lncRNA in HCC-MSCs promoting HCC progression. Using lncRNA microarray analysis, we found that a novel lncRNA named *lncRNA–MUF* (MSC-upregulated factor) was highly induced in HCC cells by HCC-MSCs. Moreover, high *lncRNA–MUF* expression was associated with poor prognosis of HCC patients. Loss- or gain-of-function analysis indicated that *lncRNA–MUF* promoted tumorigenesis and epithelial–mesenchymal transition (EMT) associated traits. Mechanistically, we found that *lncRNA–MUF* associated with Annexin A2 (ANXA2) to activate the Wnt/β-catenin signaling, consequently accelerating the EMT program. Furthermore, RNA immunoprecipitation (RIP) and RNA pulldown indicated that *lncRNA–MUF* can act as competing endogenous RNA (ceRNA) of *miR-34a*, thus allowing upregulation of Snail1 and subsequently activation of the EMT process. Collectively, our findings present the first evidence that lncRNA can play a pivotal role in MSC-mediated HCC progression.

Materials and Methods

Cell culture

293T, Hep3B, and PLC were obtained from ATCC. Huh7 from Health Science Research Resources Bank. HepG2 from the National Platform for Experimental Cell Resources. MHCC-97L, HCC-LM3, and SMMC-7721 from the Cell Bank of Shanghai Institute of Cell Biology, Chinese Academy of Sciences. Tumor cells were maintained in high glucose DMEM supplemented with 10% FBS, 100 μg/mL penicillin and 100 U/mL streptomycin. Cell lines were verified by PCR (SV40gp6 for 293T cells; HBVgp2 for PLC cells; AFP, ALB, HBVgp2 and A2M for Hep3B; AFP for Huh7 cells) and were not contaminated by mycoplasma.

Isolation of HCC-MSCs

HCC-MSCs were extracted as reported previously (3). HCC-MSCs characterization was verified by differentiation assays and surface marker analysis (19). Passages 3–10 of HCC-MSCs were used.

Transwell coculture system

Confluent HCC-MSCs were pretreated with 10 μg/mL mitomycin C for 1.5 hours. Then HCC-MSCs were enzymatically dissociated and 5×10^5 HCC-MSCs were placed on the top inserts (6.5-mm diameter with polycarbonate membrane filters containing 0.4-μm pores; Corning Inc.). After culturing 24 hours, the inserts were placed into the fresh wells of ultra-low attachment plates filled with tumorsphere medium and 2,000 HCC cells. Tumor spheres were countered under stereomicroscope after 7–9 days. Sphere medium contained DMEM/F-12 supplemented with B27 (Life Technologies; 1:50), N2 (Life Technologies,1:100), 20 ng/mL EGF, 10 ng/mL bFGF, 100 U/mL penicillin, and 100 ng/mL streptomycin (19).

LncRNA microarray analysis

GFP-positive Huh7, SMMC-7721, and HepG2 cells were cocultured with HCC-MSCs: The initial plating ratio of HCC cells to HCC-MSCs was 1:3. After coculturing for 7 days, GFP-positive HCC cells were sorted with BD FACSAria II cell sorter (BD Biosciences). Total RNA was extracted by TRIzol and hybridized to the lncRNA V3.0 microarray (Agilent). The array data were subject to quality control and background subtraction by the GeneSpring software. Quantile normalization was modulated by limma package. Probes were selected to be differential expressed when fold change was greater than 2 between experimental and control group.

Bioinformatic analysis of RNA-seq data from The Cancer Genome Atlas

The data were download from The Cancer Genome Atlas (TCGA) website and DESeq2 package was used to detect differential expressed genes. Fold change ≥ 2 and P value ≤ 0.05 were set as the threshold for significantly differential expression. Hierarchical cluster analysis of differentially expression lncRNAs was performed to explore the expression pattern. The results showed that the differentially lncRNAs could distinguish between HCC samples and adjacent tissue samples.

Survival analysis of *lncRNA-MUF*

We labeled TCGA samples as "high" or "low" according to whether the expression of lncRNA-MUF was higher or lower than the median value among all samples. The log-rank test was used to measure whether the survival time was significantly different between the "high" and "low" expressed groups. The Kaplan–Meier plots were made by the R packages.

RNA pulldown assays

RNA pulldown assays were performed as described below (14). Briefly, Biotin-labeled RNAs were transcribed with Biotin RNA Labeling Mix and T7 RNA polymerase, purified with the RNeasy Mini Kit. Total RNA was heated and annealed to form secondary structure, mixed with cytoplasm extract in RIP buffer at room temperature for 1 hour. Streptavidin agarose beads were incubated at room temperature for 1 hour. Beads were extracted by TRIzol reagent for quantitative PCR (qPCR) analysis.

In vivo tumorigenesis assays

A total of 2×10^6 tumor cells were injected subcutaneously into nude mouse. After 4 weeks, when subcutaneous tumors reached about 1 cm in diameter, mice were sacrificed, tumors were harvested, weighed, and stained with hematoxylin and eosin. The animal studies have been conducted in accordance with an Institutional Animal Care and Use Committee of Institute of Biophysics, Chinese Academy of Sciences.

Statistical analysis

Values are shown as the mean ± SD and all experiments were conducted at least three times. Significance was determined using the two tailed Student t test: *, $P < 0.05$; **, $P < 0.01$. Other methods are detailed in the Supplementary Materials and Methods.

Results

HCC-MSCs promote liver cancer stemness and tumorigenesis

Cancer-associated MSCs are becoming increasingly appreciated as an important part of the tumor microenvironment (20), but the role of HCC-MSCs in HCC progression has been less reported. Here, we found that HCC-MSCs significantly enhanced tumor sphere formation of HCC cells via Transwell coculture system (Fig. 1A). We investigated the effects of the interaction between HCC-MSCs and HCC cells (GFP). Flow cytometry analysis showed that cancer stem cell (CSC) markers such as CD90 and CD13 were significantly induced by HCC-MSCs (Fig. 1B). To further evaluate the CSC-promoting effects of HCC-MSCs *in vivo*, limiting dilution tumorigenicity assays were performed by subcutaneously inoculating luciferase-labeled SMMC-7721 cells in

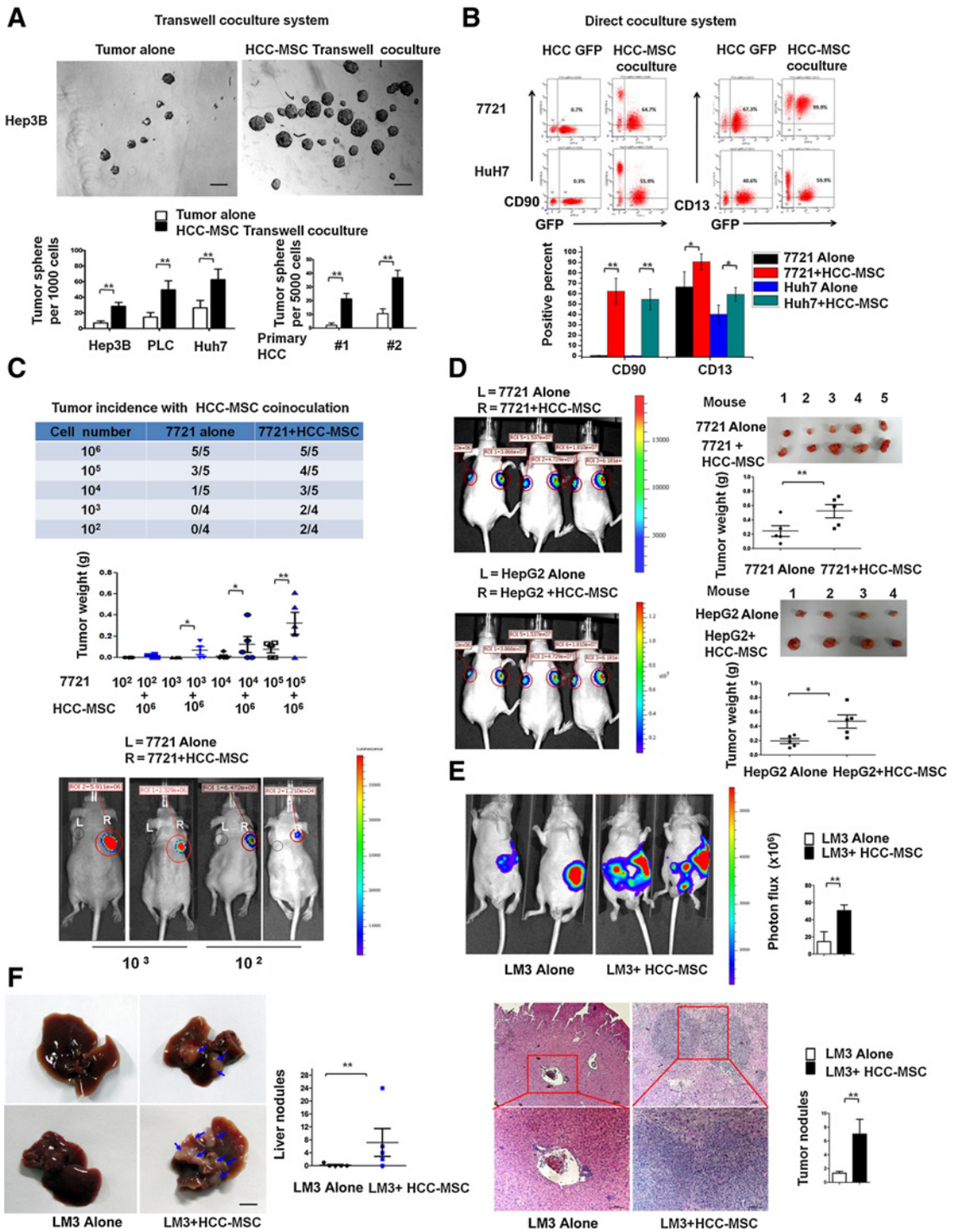

Figure 1.

HCC-MSCs promote liver cancer stemness and tumorigenesis. **A,** HCC-MSCs promoted tumor sphere formation of HCC cell lines and primary cells in the Transwell coculture system. Representative tumor spheres are from Hep3B cells cocultured with HCC-MSCs or not ($n = 3$). **B,** Flow cytometry showed that CD90- and CD13-positive population of HCC cells (GFP) was significantly enhanced when cocultured with HCC-MSCs. **C,** Luciferase-expressing SMMC-7721 cells (10^2,10^3,10^4,10^5) mixed in the absence or presence of HCC-MSCs were subcutaneously implanted into nude mice. **D,** 10^6 SMMC-7721 or HepG2 cells admixed or not with HCC-MSCs were subcutaneously injected into nude mice. Luciferase activity and tumor weights were examined to analyze the effect of HCC-MSCs on tumor formation ($n = 5$). **E,** Luciferase-expressing LM3 cells alone or with HCC-MSCs were injected into the spleen of nude mice. A representative image of metastasis *in vivo* is shown ($n = 10$). **F,** Tumor metastatic nodule in the liver. Arrows, liver metastatic nodules. Representative images show liver metastatic foci in hematoxylin and eosin–stained sections. Data are represented as the mean ± SD. Significance was determined by the two-tailed Student *t* test; $n = 3$; *, $P \leq 0.05$; **, $P \leq 0.01$.

nude mice, admixed with HCC-MSCs or not. We found that 100 or 1,000 SMMC-7721 cells alone cannot form tumor, and even 10^4 SMMC-7721 cells alone only formed tumors in 1 of 5 mice. When coinoculated with HCC-MSCs, 100 and 1,000 SMMC-7721 cells resulted in tumor formation in 2 of 4 mice (Fig. 1C). When 1×10^6 SMMC-7721 or HepG2 cells were subcutaneously inoculated, tumor weights in the HCC-MSC coinoculation group were significantly enhanced (Fig. 1D). Furthermore, both the bioluminescence intensity and metastatic nodules at liver sites indicated that HCC-MSCs significantly promoted metastasis *in vivo* (Fig. 1E and F). These results provide strong evidence that the HCC cells switch to a more aggressive phenotype when cocultured with HCC-MSCs.

LncRNA–MUF in HCC cells is significantly upregulated by HCC-MSCs

To understand the mechanism of how HCC-MSCs promote HCC progression, we used microarray analysis to evaluate changes in lncRNAs and mRNAs in HCC cells cocultured with HCC-MSCs (Fig. 2A). Transcriptome profiling identified that 57 lncRNA transcripts (Fig. 2B; Supplementary Table S1) and 110 mRNAs (Supplementary Table S1; Supplementary Fig. S1A) were differentially expressed in three different HCC cell lines when cocultured with HCC-MSCs. The transcriptome data have been deposited in the Gene Expression Omnibus (GEO) database (GSE86160). Until now most lncRNAs still remain uncharacterized, we first investigated the altered mRNAs of HCC cells induced by HCC-MSCs. Gene Set Enrichment Analysis (GSEA) and Gene Ontology (GO) assays both indicated that the differentially expressed mRNAs enriched in extracellular matrix, which is closely associated with the EMT signaling (21) and metastasis (Supplementary Fig. S1B–S1D; ref. 22). In addition, qPCR and Western blotting assays confirmed that EMT-related genes were significantly upregulated by HCC-MSC conditioned medium (Supplementary Fig. S1E and S1F). TGF-β1, a well-characterized inducer of EMT, served as the positive control (Supplementary Fig. S1G). Our results suggest that HCC-MSCs might largely promote HCC malignancy through the EMT process.

To further identify which lncRNAs might play important roles in HCC-MSCs promoting HCC progression, candidate lncRNAs were screened using the following criteria: lncRNA expression was significantly altered by HCC-MSCs in lncRNA microarrays (Fig. 2B, Supplementary Table S1) and TCGA database, indicating differential expression of the lncRNAs in HCC specimens compared with adjacent nontumor tissues (Fig. 2C). Among the five most differentially expressed lncRNAs, a novel lncRNA (*LINC00941*, Ensembl ID: ENSG00000235884, fold changes >5 and $P < 0.01$) particularly drew our attention (Fig. 2D). As this is an uncharacterized lncRNA, we termed it *lncRNA–MUF* (MSCs upregulated factor). Consistent with the microarray results, qPCR assays confirmed that *lncRNA–MUF* was significantly upregulated in HCC cells by HCC-MSCs (Supplementary Fig. S2A and S2B). In addition, it was highly expressed in HCC specimens compared with adjacent nontumor tissues (Fig. 2E). The TCGA data (Fig. 2F) and our previous lncRNA microarray (GSE70880, Supplementary Fig. S2C) confirmed these results (23, 24). Notably, Kaplan–Meier survival analysis indicated that high *lncRNA-MUF* expression was correlated with poor survival of HCC patients (Fig. 2F). Furthermore, *lncRNA–MUF* expression was significantly enhanced by HCC-MSC conditioned medium and TGF-β1 (Fig. 2G; Supplementary Fig. S2D). Moreover, *lncRNA-MUF* was highly expressed in tumor spheres and highly invasive HCC cells (Fig. 2G). Collectively, these findings indicate that *lncRNA–MUF* is significantly upregulated by HCC-MSCs.

LncRNA–MUF is required for tumor sphere formation and the EMT process

LncRNA–MUF resides on chromosome 12p11.21 and is localized near active regulatory elements including the histone mark H3K27Ac marks and DNaseI hypersensitivity clusters (Fig. 3A). A 1884-base pair (bp) transcript was determined by 5′ and 3′ rapid amplification of cDNA ends assays (RACE) and displayed no coding potential, as determined by the CNCI, CPAT, and PhyloCSF score analysis (Supplementary Table S2). Northern blot assays confirmed that one transcript of about 1,800 bp was mainly found in HCC cells (Supplementary Fig. S2E). Cellular fractionation and RNA FISH (RNA-FISH) analysis indicated that *lncRNA–MUF* was mainly localized in the cytoplasm (Fig. 3B). Knockdown of *lncRNA–MUF* significantly attenuated the capacity of tumor sphere formation and invasion *in vitro* (Fig. 3C; Supplementary Fig. S2F). Moreover, *lncRNA–MUF* depletion significantly repressed the subcutaneous xenograft formation and metastatic capacity *in vivo* (Fig. 3D). In contrast, tumor sphere formation was increased in *lncRNA–MUF*–overexpressing cells (Fig. 3E). Given the fact that HCC-MSCs stimulate the EMT process, we examined the expression of EMT-related gene after *lncRNA–MUF* alteration. Both qPCR and Western blotting demonstrated that *lncRNA–MUF* depletion significantly repressed the expression of mesenchymal-related genes, whereas *lncRNA–MUF* overexpression had the opposite effect (Fig. 3F). Taken together, these data show that *lncRNA–MUF* can regulate the EMT program to promote HCC progression.

LncRNA-MUF interacts with ANXA2

LncRNAs can exert their functions through RNA–protein interactions to modulate target genes (12, 25). Therefore, we used RNA pulldown assays followed by silver staining and mass spectrometry (MS) to identify *lncRNA–MUF*–protein interactions. ANXA2 was found to specifically bind to *lncRNA–MUF* (Fig. 4A; Supplementary Table S3). As shown in Fig. 4B, ANXA2 was detected in the biotin-labeled sense *lncRNA–MUF* group through RNA pulldown assays followed by Western blotting. Moreover, the interactions between *lncRNA–MUF* and ANXA2 were verified by RNA immunoprecipitation (RIP) assays (Fig. 4C). In addition, a series of truncated *lncRNA–MUF* were constructed to map the specific binding region between *lncRNA–MUF* and ANXA2, suggesting that nucleotides 800 to 1,600 of *lncRNA-MUF* could bind to ANXA2 (Fig. 4D). Competitive RNA pulldown assays further confirmed the interaction of ANXA2 with *lncRNA–MUF* (Fig. 4E). Moreover, RNA-FISH and immunofluorescence assays indicated that *lncRNA–MUF* colocalized with ANXA2 in the cytoplasm of HCC cells (Fig. 4F). The GEO data showed that *ANXA2* was highly expressed in HCC tissues and metastatic samples (Fig. 4G). Depletion of *ANXA2* significantly repressed tumor sphere formation and tumorigenicity (Fig. 4H). These data indicate that *lncRNA–MUF*–ANXA2 axis can modulate HCC progression.

LncRNA–MUF interacts with ANXA2 to activate the Wnt/β-catenin signaling

To investigate the mechanism by which the *lncRNA–MUF*–ANXA2 axis promotes HCC progression, we examined the expression of EMT-related genes upon *ANXA2* alteration. Mesenchymal-

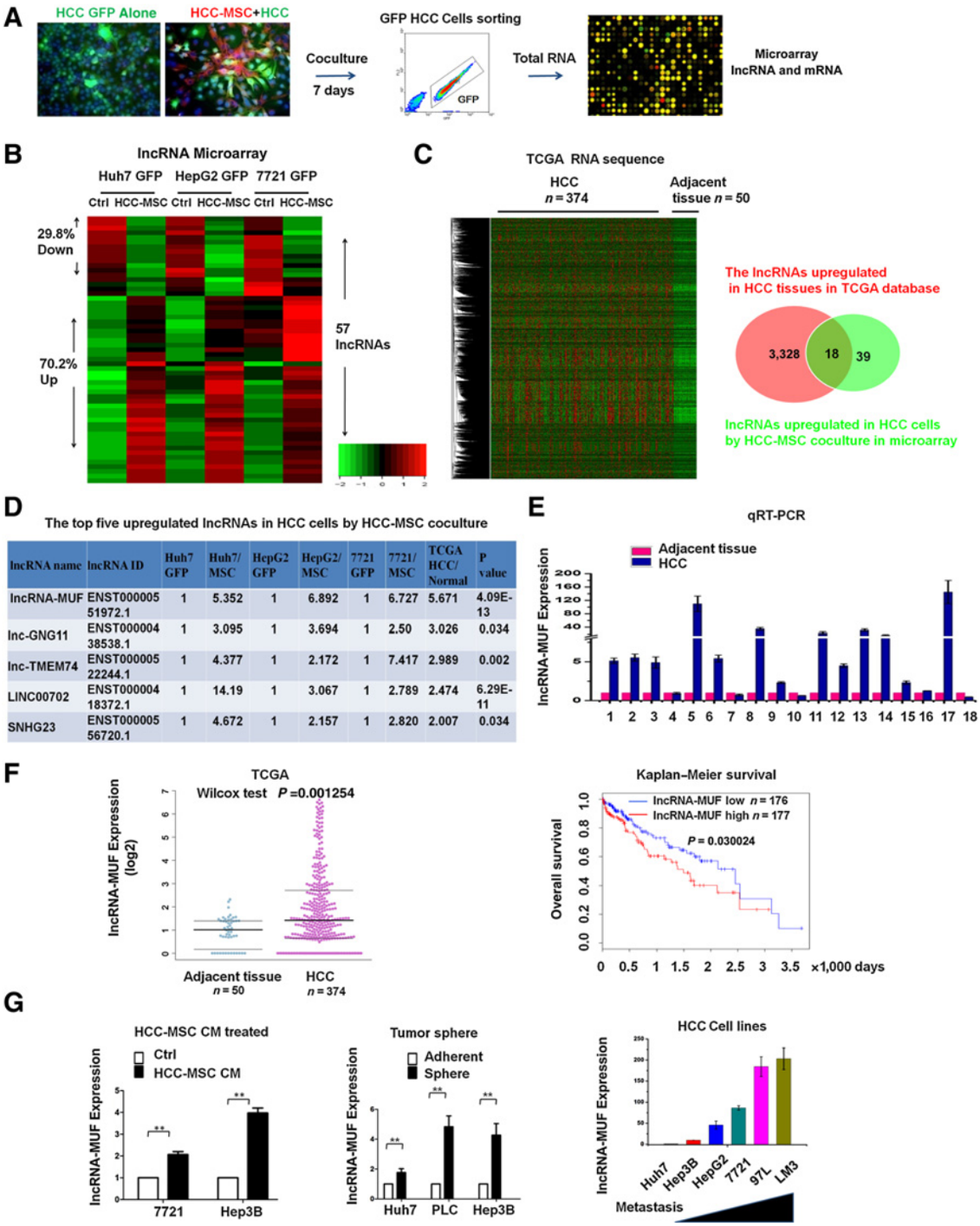

lncRNA name	lncRNA ID	Huh7 GFP	Huh7/ MSC	HepG2 GFP	HepG2/ MSC	7721 GFP	7721/ MSC	TCGA HCC/ Normal	P value
lncRNA-MUF	ENST00000551972.1	1	5.352	1	6.892	1	6.727	5.671	4.09E-13
lnc-GNG11	ENST00000438538.1	1	3.095	1	3.694	1	2.50	3.026	0.034
lnc-TMEM74	ENST00000522244.1	1	4.377	1	2.172	1	7.417	2.989	0.002
LINC00702	ENST00000418372.1	1	14.19	1	3.067	1	2.789	2.474	6.29E-11
SNHG23	ENST00000556720.1	1	4.672	1	2.157	1	2.820	2.007	0.034

Figure 2.

LncRNA alterations of HCC cells when interacted with HCC-MSCs. **A,** Schematic overview of the experimental design. HCC cells (GFP) cocultured with HCC-MSCs or not were sorted by flow cytometry and analyzed by microarray. **B,** Altered lncRNA expression in HCC cells when cocultured with HCC-MSCs. Expression values above or below the global median scale are represented in shades of red and green, respectively. **C,** Merged upregulated lncRNAs in the TCGA database (HCC samples vs. adjacent nontumor tissues) and our microarray (HCC-MSCs coculture vs. HCC cells alone). **D,** The five most upregulated lncRNAs of HCC cells when cocultured with HCC-MSCs. **E,** qPCR assays indicated that *lncRNA–MUF* was significantly upregulated in HCC specimens compared with adjacent non-tumor tissues ($n = 3$). **, $P < 0.01$. **F,** The TCGA database indicated that *lncRNA–MUF* is highly expressed in HCC tissues and is correlated with poor survival by Kaplan–Meier survival analysis. $P = 0.030024$. **G,** *LncRNA–MUF* expression was further analyzed in HCC cells when treated with HCC-MSCs conditioned medium, tumor spheres, and HCC cell lines. Data are presented as the mean ± SD. Significance was determined by the two-tailed Student *t* test; $n = 3$; *, $P \leq 0.05$; **, $P \leq 0.01$.

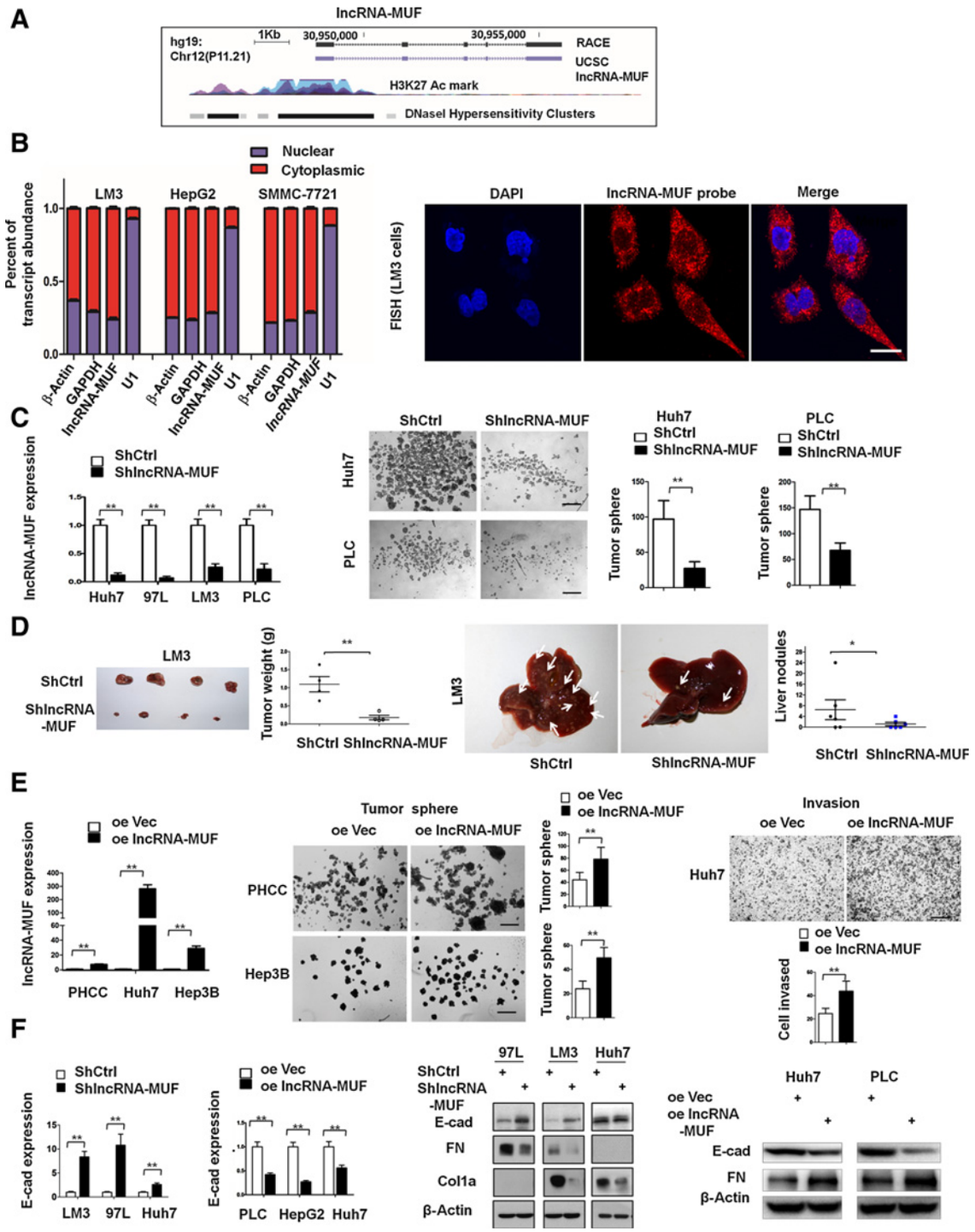

Figure 3.

LncRNA–MUF is required for tumor sphere formation and the EMT process. **A,** Schematic annotation of the *lncRNA-MUF* genomic locus. **B,** Fractionation of HCC cells followed by qPCR assays were used to determine the localization of *lncRNA–MUF*. *GAPDH* and *β-actin* served as the control for cytoplasmic expression, and *U1* was the control for nuclear expression. RNA-FISH assays were used to confirm *lncRNA–MUF* localization. DAPI, 4′, 6-diamidino-2-phenylindole. Probes, DIG-labeled *lncRNA-MUF*; $n = 3$; scale bar, 10 μm. **C,** *LncRNA–MUF* depletion significantly reduced tumor sphere formation. **D,** Tumor formation and metastasis were significantly decreased in *lncRNA–MUF* knockdown cells. **E,** *LncRNA–MUF* overexpression significantly enhanced tumor sphere formation and invasion of HCC cells. **F,** qPCR and Western blotting assays were used to detect the alteration of the EMT process when *lncRNA–MUF* was depleted or overexpressed. Data are presented as the mean ± SD. Significance was determined by the two-tailed Student *t* test; $n = 3$; *, $P \leq 0.05$; **, $P \leq 0.01$.

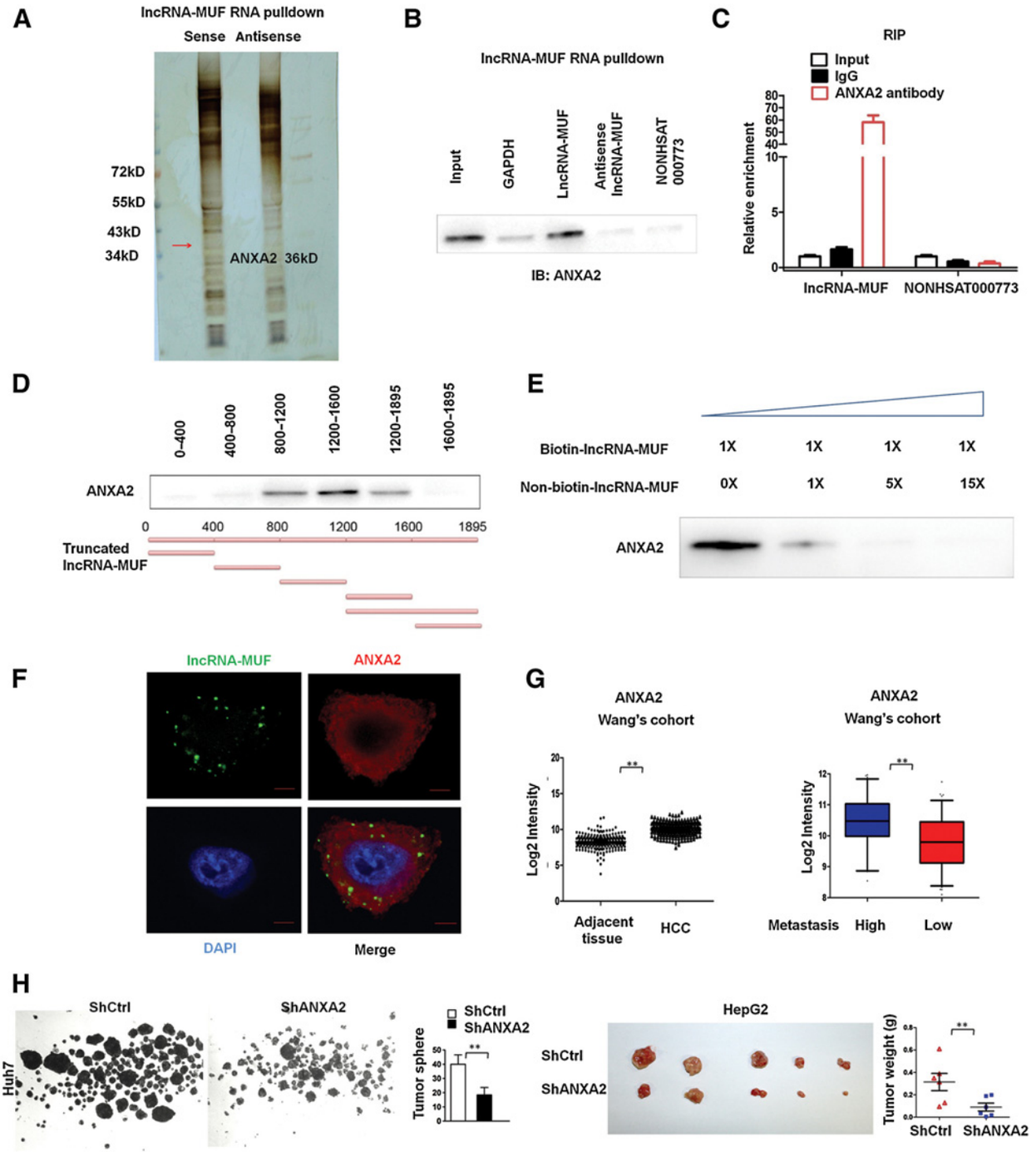

Figure 4.

Interaction of *lncRNA–MUF* and ANXA2. **A,** RNA pulldown assays were performed using biotin-labeled sense or antisense *lncRNA–MUF*. Silver staining and mass spectrometry were performed to identify the interacting proteins. Red arrow, the ANXA2 band. **B,** Proteins were pulled down by biotin-labeled sense or antisense *lncRNA–MUF* and analyzed by immunoblotting with the ANXA2 antibody. **C,** RIP assays were performed with ANXA2 antibody, followed by qPCR to enrich *lncRNA-MUF*. **D,** RNA pulldown assays were performed with a series of truncated *lncRNA–MUF* variants and followed by immunoblotting with the ANXA2 antibody. **E,** Competition assays using biotin-labeled and unlabeled *lncRNA–MUF* confirmed the binding of *lncRNA–MUF* with ANXA2. **F,** *LncRNA–MUF* (green) was visualized by RNA-FISH assays and ANXA2 (red) was detected by immunofluorescence. Nucleus was stained with DAPI (blue). **G,** *ANXA2* was highly expressed in metastatic HCC tissues and HCC samples using Wang's cohort (GSE14520). **H,** *ANXA2* depletion significantly suppressed the proliferation of tumor sphere *in vitro* and tumor formation *in vivo*. Data are presented as the mean ± SD. Significance was determined by the two-tailed Student *t* test; $n = 3$; *, $P \leq 0.05$; **, $P \leq 0.01$.

related genes and β-catenin were significantly altered by *ANXA2* overexpression or knockdown (Fig. 5A). β-Catenin in different cellular compartments mediates distinct cellular function (26), thus we determined whether *ANXA2* affected the subcellular distribution of β-catenin. As shown in Fig. 5B, Western blotting assays showed an increase of β-catenin in the cytosol and nucleus of *ANXA2*-overexpressing cells. In contrast, β-catenin in the nucleus decreased substantially in *ANXA2*-knockdown cells. Furthermore, several β-catenin target genes were upregulated in *ANXA2*-overexpressing cells and downregulated in *ANXA2* knockdown cells (Supplementary Fig. S3A). These results suggest that *ANXA2* can alter the subcellular localization of β-catenin to activate the Wnt cascade. Phosphorylation of β-catenin by glycogen synthase kinase 3β (GSK-3β) causes its degradation by the ubiquitin-proteasome system (27). Therefore, we examined whether the altered expression of β-catenin resulted from phosphorylation by GSK-3β. As shown in Fig. 5A, phosphorylation of β-catenin at S33/S37 and T41 residues was reduced in *ANXA2*-overexpressing cells and increased in *ANXA2* knockdown cells. Coimmunoprecipitation (co-IP) assays showed that GSK-3β precipitated less endogenous β-catenin in ANXA2-overexpressing cells (Fig. 5C) and more β-catenin in ANXA2-knockdown cells (Fig. 5D). Likewise, endogenous GSK-3β precipitated by β-catenin were affected by ANXA2 alterations (Fig. 5C and D). Furthermore, co-IP and RNA-FISH assays showed that ANXA2 could bind with GSK-3β (Fig. 5E; Supplementary Fig. S3B) but not directly interact with β-catenin (Supplementary Fig. S3C). Taken together, these results show that ANXA2 can bind to GSK-3β and disrupt the formation of the GSK-3β/β-catenin complex. Moreover, we investigated the effect of *lncRNA–MUF* in the interaction between GSK-3β and ANXA2, and found that knockdown of *lncRNA–MUF* repressed the promoting effect of ANXA2 on β-catenin and EMT-related proteins (Fig. 5F). In addition, co-IP assays confirmed that *lncRNA-MUF* overexpression significantly enhanced the interactions between ANXA2 and GSK-3β, whereas *lncRNA–MUF* depletion repressed the binding effect (Fig. 5G). Analysis of *lncRNA–MUF* truncations indicated that GSK-3β but not β-catenin binds to nucleotides 800 to 1,200 of *lncRNA–MUF* (Supplementary Fig. S3D), showing that *lncRNA–MUF* interacts with ANXA2 and GSK-3β via distinct but partially overlapping domains. Taken together, the binding of *lncRNA–MUF* and ANXA2 plays important roles in the activation of Wnt/β-catenin signaling and the EMT process.

LncRNA–MUF promotes HCC progression by acting as a ceRNA of miR-34a

Emerging evidence suggests that cytoplasmic lncRNAs can act as ceRNAs to modulate the functions of miRNAs (15, 28, 29). To examine whether cytoplasmic localized *lncRNA–MUF* can bind endogenous miRNAs, we predicted the target miRNAs using PITA and RNAhybrid softwares. Only the miRNAs with highly ranking target sites and low expression in HCC tissues were selected for further analysis (Supplementary Fig. S4A). RIP and RNA pull-down assays showed that *miR-34a* and *miR-133a* were significantly enriched in the *lncRNA–MUF* group compared with the control (Fig. 6A and B). Our preliminary results showed that *miR-34a* repressed tumor sphere formation more significantly than *miR-133a* (data not shown). Thus, we mainly focused on the effect of *lncRNA–MUF* binding to *miR-34a*. Luciferase activities and AGO_2 RIP assays showed that *lncRNA-MUF* could bind with *miR-34a* (Fig. 6C). Furthermore, RNA-FISH analysis demonstrated that *lncRNA–MUF* was colocalized with *miR-34a* in the cytoplasm of HCC cells (Fig. 6D). Next, we found that miR-34a repressed tumor sphere formation and tumor growth of HCC cells (Supplementary Fig. S4B and S4C). Moreover, when *lncRNA–MUF* and *miR-34a* were cotransfected into HCC cells, *lncRNA-MUF* significantly rescued the inhibitory role of *miR-34a* on tumor sphere formation and invasion (Fig. 6E; Supplementary Fig. S4D). In addition, qPCR and Western blotting analysis showed that *lncRNA–MUF* could recover the inhibitory effect of *miR-34a* on the EMT process (Fig. 6F). These data indicate that *lncRNA–MUF* acts as a ceRNA to affect the function of miR-34a in HCC cells.

The *lncRNA–MUF–miR-34a* axis promotes HCC malignancy through Snail1

To further elucidate the mechanism underlying the contribution of the *lncRNA–MUF–miR-34a* axis to HCC progression, TargetScan software predicted that *Snail1* was one of the targets of *miR-34a* (Fig. 7A). And *miR-34a* significantly repressed the expression of Snail1 in HCC cells; luciferase reporter assays demonstrated that *miR-34a* could bind the 3′-untranslated region (UTR) of *Snail1*. Importantly, *lncRNA–MUF* attenuated the binding capacity of *miR-34a* to the 3′-UTR of *Snail1* (Fig. 7A). Moreover, Western blotting analysis confirmed that *lncRNA–MUF* could reduce the inhibitory effect of *miR-34a* on Snail1 expression (Fig. 7B). In addition, *Snail1* knockdown suppressed tumor sphere formation induced by *lncRNA-MUF* overexpression (Fig. 7C). qPCR and Western blotting analysis demonstrated that *Snail1* depletion inhibited the promoting effect of *lncRNA-MUF* on the EMT progress (Fig. 7D and E). Taken together, these data show that *lncRNA–MUF* can function as a ceRNA of *miR-34a* to regulate the expression of Snail1 and enhance the EMT process.

A schematic representation of the cross-talk between HCC-MSCs and HCC cells is illustrated in Fig. 7F. The interaction between HCC-MSCs and HCC cells induced the upregulation of *lncRNA–MUF*, thereafter, *lncRNA–MUF* can associate with ANXA2 and miR-34a to regulate the EMT process and tumor progression.

Discussion

In this study, we investigated the role of lncRNAs in HCC-MSCs promoting HCC progression. Interestingly, we found that the novel *lncRNA–MUF* was significantly increased in HCC cells by HCC-MSCs. Moreover, *lncRNA–MUF* significantly promoted tumorigenesis and EMT traits. Mechanistically, *lncRNA–MUF*-interacted with ANXA2 and *miR-34a* to participate in the EMT process and tumorigenesis. Collectively, the results of this study present a new mechanism by which HCC-MSCs promote HCC progression.

Recent studies have indicated that tumorigenesis relies heavily on the reciprocal interactions between tumor cells and the surrounding stroma (30–33). Identifying the critical pathway involved in this cross-talk could potentially improve the efficiency of treatment (34, 35). It has been increasingly recognized that cancer-associated MSCs act as important contributors to tumor progression (20, 36). However, most studies have focused on the role of growth factors or cytokines in the cross-talk between MSCs and tumor cells. Breast cancer–associated MSCs promoted sphere formation via the EGF/EGFR/Akt pathway (19). McLean and colleagues (36) demonstrated that ovarian cancer–associated MSCs expressed more bone morphogenetic proteins, thereby

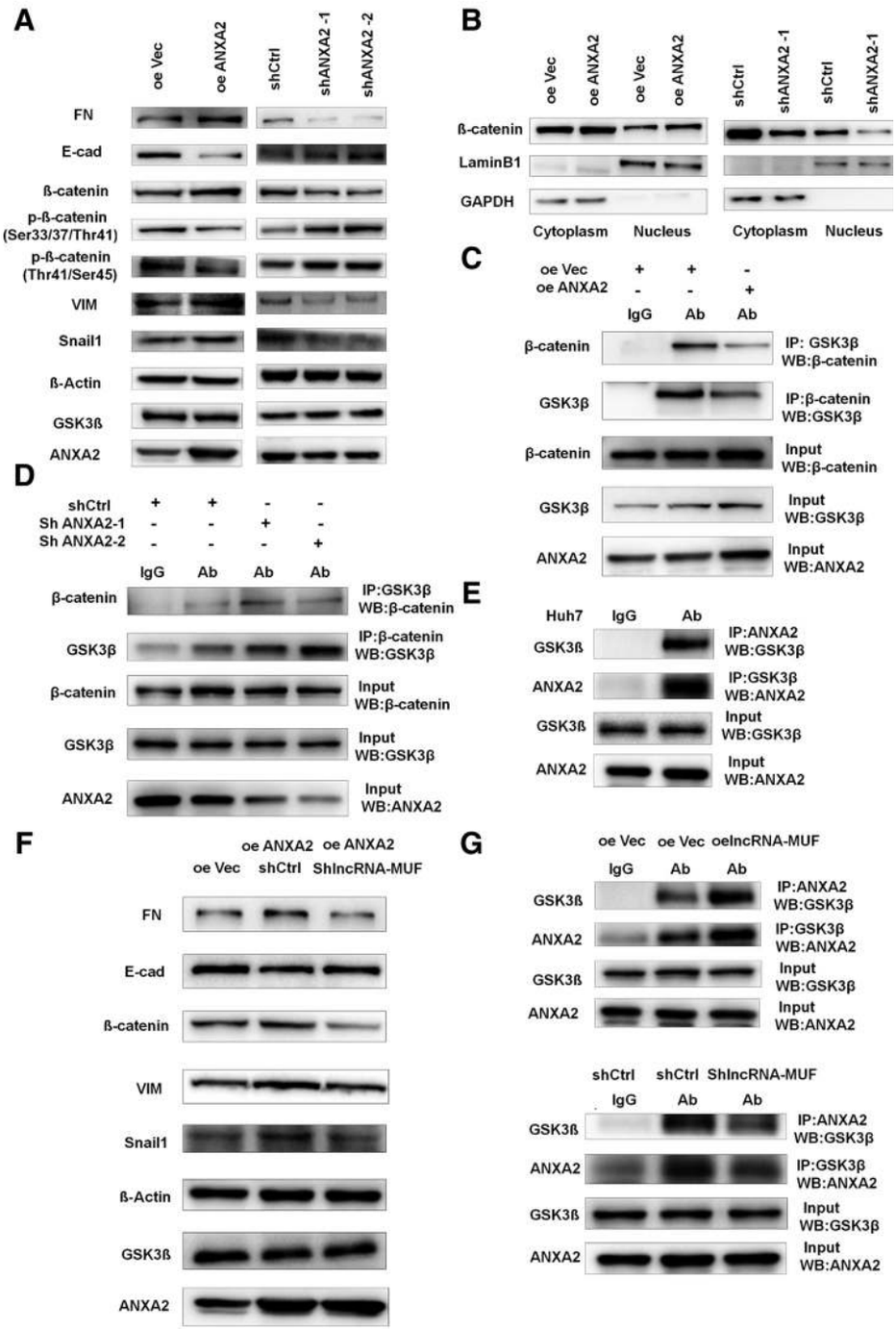

Figure 5.

LncRNA–MUF associates with ANXA2 to activate Wnt/β-catenin signaling and the EMT process. **A,** Wnt/β-catenin signaling and the EMT pathway were investigated in *ANXA2* overexpression and depletion cells by Western blotting. **B,** Cytosolic and nuclear proteins were isolated from *ANXA2*-overexpression cells and analyzed with the β-catenin antibody. GAPDH and LaminB1 were used as positive controls of cytosolic and nuclear fraction, respectively. **C** and **D,** Co-IP assays were performed with GSK-3β or β-catenin antibody in *ANXA2*-overexpressing cells (**C**) or knockdown cells (**D**). **E,** Co-IP assays showed that ANXA2 could interact with GSK-3β. **F,** Western blotting analysis was utilized to examine the effect of *lncRNA–MUF* depletion on the EMT pathway in *ANXA2*-overexpression cells. **G,** The interactions between ANXA2 and GSK-3β were investigated by co-IP analysis in *lncRNA–MUF*-overexpression or knockdown cells. Data are presented as the mean ± SD. Significance was determined by the two-tailed Student *t* test; $n = 3$; *, $P \leq 0.05$; **, $P \leq 0.01$.

altering the stemness of ovarian tumors. Waghray and colleagues (20) indicated that pancreatic adenocarcinoma-associated MSCs can secret more granulocyte macrophage-colony stimulating factor to enhance tumor proliferation. Our previous results demonstrated that S100A4 secreted from HCC-MSCs could participate in HCC progression (3). Recently, accumulating evidence has suggested that dysregulated lncRNAs are involved in the proliferation (16, 37), metastasis (17), CSCs maintenance (38), and prognosis of HCC patients (39). However, it has remained unknown whether lncRNAs can play roles in the cross-talk between HCC-MSCs and HCC cells.

In this study, we used mRNA and lncRNA microarrays to investigate the mechanism of the interactions between HCC-MSCs and HCC cells. We firstly analyzed the altered mRNAs in HCC cells by HCC-MSCs, GSEA, and GO analyses indicated that HCC-MSCs conferred EMT characteristics to HCC cells. The EMT causes epithelial cells to acquire mesenchymal traits and is closely associated with CSC-like features (21, 22, 40). In accordance with

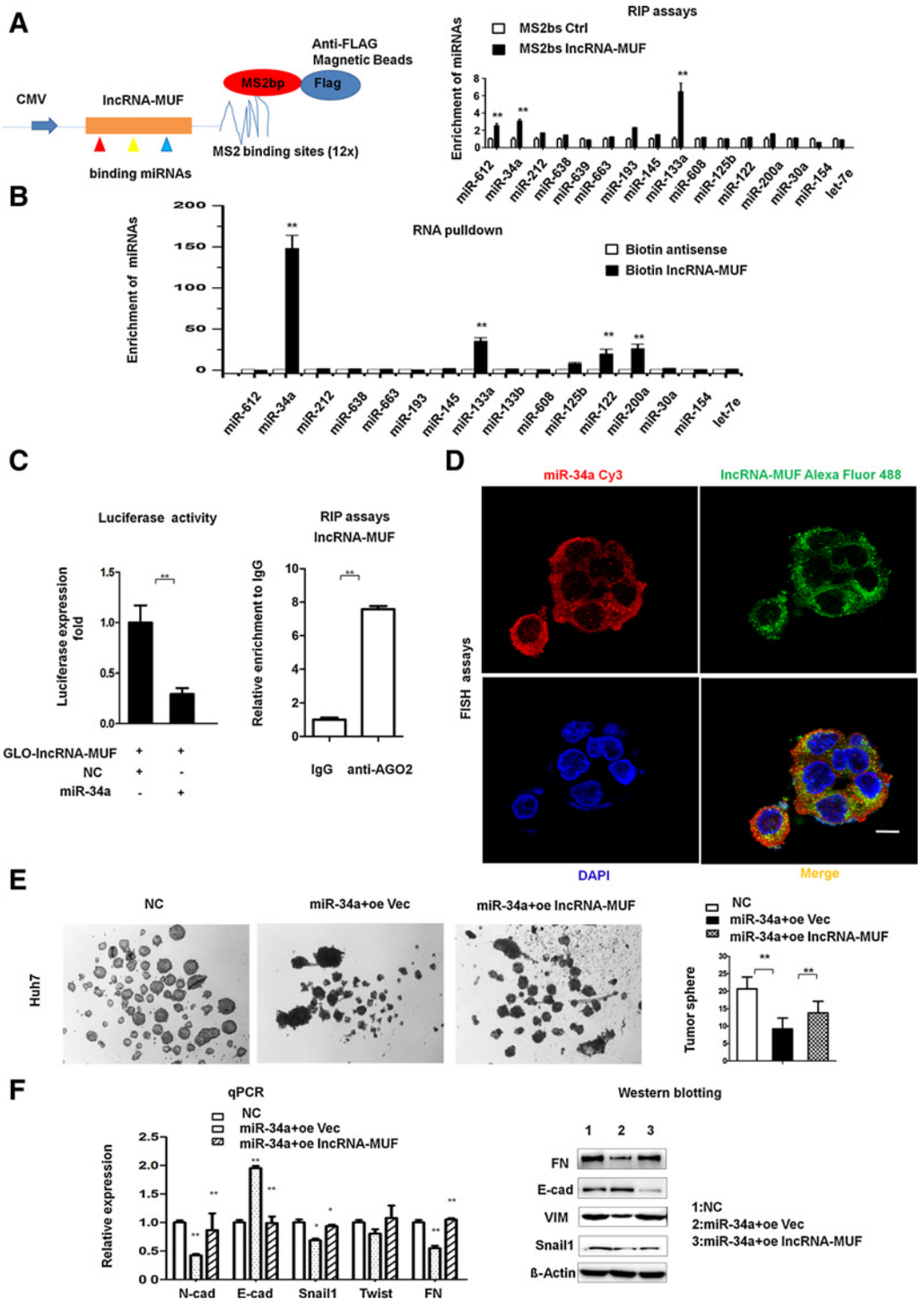

Figure 6.

LncRNA–MUF acts as a ceRNA of *miR-34a* to promote the EMT process. **A,** Schematic representation of the MS2-RIP assays, followed by qPCR to detect the endogenous miRNAs associated with *lncRNA–MUF*. **B,** Enriched miRNAs were verified via RNA pulldown assays with biotin-labeled sense or antisense *lncRNA–MUF*. **C,** Luciferase activity assays demonstrated that *lncRNA–MUF* could bind with *miR-34a*. Moreover, RNA pulldown assays with anti-AGO2 was performed in *miR-34a*–overexpressing Huh7 cells, followed by qPCR to enrich *lncRNA–MUF*. **D,** Representative image of RNA-FISH assays indicated the colocalization of *lncRNA–MUF* (green dots) and *miR-34a* (red dots) in HCC cells; scale bar, 5 μm. **E,** *LncRNA–MUF* overexpression attenuated the inhibitory role of *miR-34a* on tumor sphere formation. **F,** qPCR and Western blotting analysis demonstrated that *lncRNA–MUF* overexpression could inhibit the repressive effect of *miR-34a* on the EMT process. Data are presented as the mean ± SD. Significance was determined by the two-tailed Student *t* test; $n = 3$; *, $P \leq 0.05$; **, $P \leq 0.01$.

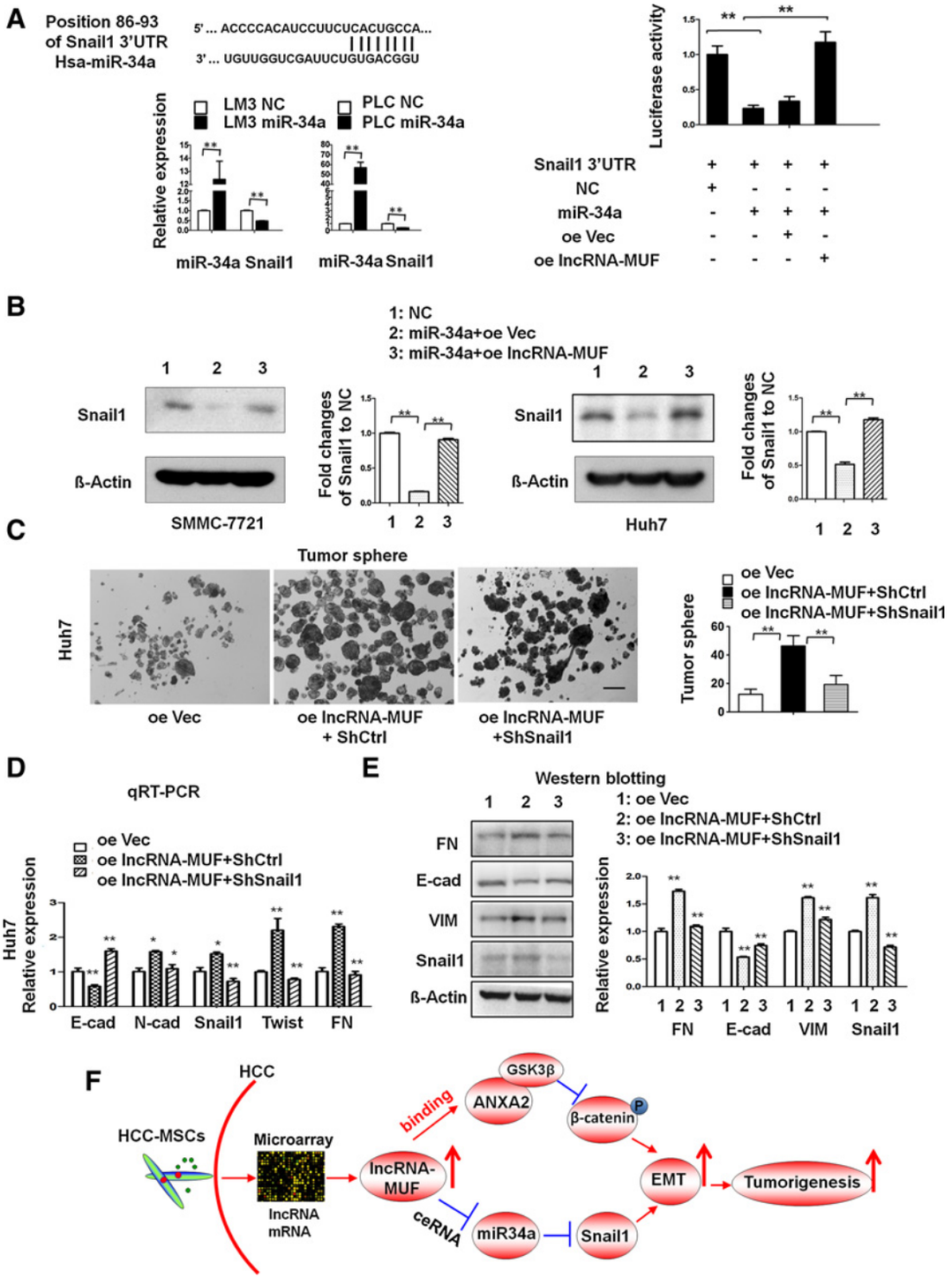

Figure 7.

The *lncRNA–MUF–miR-34a* axis promoted HCC malignancy via Snail1. **A,** TargetScan software predicted that Snail1 was one of the targets of *miR-34a*. qPCR assays demonstrated that *miR-34a* overexpression repressed the expression of Snail1. Dual-luciferase reporter assays further confirmed that *lncRNA–MUF* could compete with *miR-34a* to bind the 3′-UTR of Snail1. **B,** Western blotting showed that *miR-34a* repressed the expression of Snail1, whereas *lncRNA–MUF* overexpression partially counteracted these inhibitory effects. **C,** *Snail1* depletion significantly repressed the promoting effect of *lncRNA–MUF* on tumor sphere formation. **D** and **E,** qPCR and Western blotting analysis showed that *Snail1* depletion blocked the promoting effect of *lncRNA–MUF* on the EMT process. Data are presented as the mean ± SD. Significance was determined by the two-tailed Student *t* test; $n = 3$. *, $P \leq 0.05$; **, $P \leq 0.01$. **F,** Schematic representation illustrates that HCC-MSCs can modulate HCC progression via upregulating the expression of *lncRNA–MUF*, which can associate with ANXA2 and *miR-34a* to accelerate the EMT process and tumorigenesis.

the role of HCC-MSCs in liver cancer progression as well as inducing the EMT in HCC cells, we hypothesized that the differentially expressed lncRNAs induced by HCC-MSCs might play important roles in modulating the EMT program.

Through screening of our microarrays and the TCGA data, we found that *lncRNA–MUF* was one of the most highly expressed lncRNAs in HCC cells induced by HCC-MSCs and it played a critical role in EMT modulation. Through RNA pulldown and mass spectrometry analyses, ANXA2 was found to bind with *lncRNA–MUF*, and the binding led to upregulated β-catenin and the EMT process. Upregulation of β-catenin occurs in several cancers such as colorectal cancer (41), breast cancer (42), and liver cancer (43). Canonical Wnt signaling depends on β-catenin/GSK-3β complex conformation and phosphorylation by GSK-3β, leading to β-catenin degradation (44, 45). Our results showed that ANXA2 could bind to GSK-3β and disrupt the formation of GSK-3β/β-catenin complex. In addition, co-IP experiments showed that *lncRNA–MUF* could promote the interaction between GSK-3β and ANXA2. Our results demonstrate that *lncRNA–MUF* might play a critical role in Wnt signaling to promote HCC development.

It was recently shown that cytoplasmic-localized lncRNAs can act as ceRNAs to regulate miRNAs (29, 46). *LncRNA-ATB* activated by TGF-β1 promotes the HCC invasion-metastasis cascade by competitively binding *miR-200s* to regulate the EMT factors ZEB1 and ZEB2 (17). Exosome-transmitted *lncARSR* acts as a ceRNA of *miR-449* to facilitate c-MET expression and promote sunitinib resistance (47). The pseudogene *BRAF*, which encodes a subclass of lncRNAs, functions as ceRNAs to induce lymphoma formation (15). In our study, we found that *lncRNA–MUF* functions as a ceRNA of *miR-34a* to regulate Snail1 activity and modulate HCC progression.

In this study, we mainly focused on the downstream mechanism by which *lncRNA–MUF* participates in HCC development. However, it still remains unknown how HCC-MSCs upregulate the expression of *lncRNA–MUF*. Because HCC-MSC–conditioned medium can enhance the expression of *lncRNA–MUF*, we speculated that growth factors or cytokines secreted from HCC-MSCs may participate in the regulation of *lncRNA–MUF* expression. However, we cannot rule out the possibility that HCC-MSCs can modulate the expression of *lncRNA–MUF* via direct physical contact. It will be of great interest to explore in future studies.

In summary, our study highlights the importance of *lncRNA–MUF* as a mediator of MSC niche modulating HCC progression. To the best of our knowledge, this is the first study to characterize the role of lncRNA in the cross-talk between MSCs and HCC cells. These results provide new insights into the mechanism underlying the interactions between the tumor microenvironment and HCC cells.

Disclosure of Potential Conflicts of Interest

No potential conflicts of interest were disclosed.

Authors' Contributions

Conception and design: X. Yan, D. Zhang, S. Wu, R. Chen, Z. Fan
Development of methodology: X. Yan, D. Zhang, S. Wu, J. Qian, J. Wu, Y. Huang, X. Liu, B. Liu
Acquisition of data (provided animals, acquired and managed patients, provided facilities, etc.): X. Yan, D. Zhang, J. Qian, F. Yan, G. Huang, X. Liu
Analysis and interpretation of data (e.g., statistical analysis, biostatistics, computational analysis): X. Yan, D. Zhang, W. Wu, Y. Hao, F. Yan, P. Zhu, Y. Huang
Writing, review, and/or revision of the manuscript: X. Yan, D. Zhang, W. Wu, Z. Fan
Administrative, technical, or material support (i.e., reporting or organizing data, constructing databases): X. Yan, D. Zhang, J. Luo, X. Chen, Y. Du
Study supervision: R. Chen, Z. Fan

Acknowledgments

We are grateful to Dr. Geir Skogerbø for manuscript reading and we thank LetPub (www.letpub.com) for its linguistic assistance of the manuscript. We thank Prof. Xiaofei Zheng (Beijing Institute of Radiation Medicine, Beijing, China) for providing MS2bs plasmids and Dr. Junying Jia for FACS analysis.

Grant Support

This work was supported by grants from National Natural Science Foundation of China (81472341 and 81772617 to X. Yan; 31401098 to D. Zhang; and 31520103905 to R. Chen); Beijing Natural Science Foundation (7152095 to X. Yan); Beijing Municipal Education Commission (KM201710005031 to X. Yan); 973 Program of the MOST of China (2015CB553705 to Z. Fan); National High Technology Research and Development Program of China (2015AA020108 to R. Chen).

The costs of publication of this article were defrayed in part by the payment of page charges. This article must therefore be hereby marked *advertisement* in accordance with 18 U.S.C. Section 1734 solely to indicate this fact.

Received June 28, 2017; revised August 20, 2017; accepted September 20, 2017; published OnlineFirst September 25, 2017.

References

1. Torre LA, Bray F, Siegel RL, Ferlay J, Lortet-Tieulent J, Jemal A. Global cancer statistics, 2012. CA Cancer J Clin 2015;65:87–108.
2. El-Serag HB. Hepatocellular carcinoma. N Engl J Med 2011;365:1118–27.
3. Yan XL, Jia YL, Chen L, Zeng Q, Zhou JN, Fu CJ, et al. Hepatocellular carcinoma-associated mesenchymal stem cells promote hepatocarcinoma progression: role of the S100A4-miR155-SOCS1-MMP9 axis. Hepatology 2013;57:2274–86.
4. Shi Y, Du L, Lin L, Wang Y. Tumour-associated mesenchymal stem/stromal cells: emerging therapeutic targets. Nat Rev Drug Discov 2017;16:35–52.
5. Lo A, Wang LS, Scholler J, Monslow J, Avery D, Newick K, et al. Tumor-promoting desmoplasia is disrupted by depleting FAP-expressing stromal cells. Cancer Res 2015;75:2800–10.
6. Quante M, Tu SP, Tomita H, Gonda T, Wang SS, Takashi S, et al. Bone marrow-derived myofibroblasts contribute to the mesenchymal stem cell niche and promote tumor growth. Cancer Cell 2011;19:257–72.
7. Tondreau T, Meuleman N, Delforge A, Dejeneffe M, Leroy R, Massy M, et al. Mesenchymal stem cells derived from CD133-positive cells in mobilized peripheral blood and cord blood: proliferation, Oct4 expression, and plasticity. Stem Cells 2005;23:1105–12.
8. da Silva Meirelles L, Caplan AI, Nardi NB. In search of the *in vivo* identity of mesenchymal stem cells. Stem Cells 2008;26:2287–99.
9. Crisan M, Yap S, Casteilla L, Chen CW, Corselli M, Park TS, et al. A perivascular origin for mesenchymal stem cells in multiple human organs. Cell Stem Cell 2008;3:301–13.
10. Guttman M, Rinn JL. Modular regulatory principles of large non-coding RNAs. Nature 2012;482:339–46.
11. Yin Y, Yan P, Lu J, Song G, Zhu Y, Li Z, et al. Opposing roles for the lncRNA haunt and its genomic locus in regulating HOXA gene activation during embryonic stem cell differentiation. Cell Stem Cell 2015;16:504–16.
12. McHugh CA, Chen CK, Chow A, Surka CF, Tran C, McDonel P, et al. The Xist lncRNA interacts directly with SHARP to silence transcription through HDAC3. Nature 2015;521:232–6.
13. Bhan A, Soleimani M, Mandal SS. Long noncoding RNA and cancer: a new paradigm. Cancer Res 2017;77:3965–81.

14. Li D, Liu X, Zhou J, Hu J, Zhang D, Liu J, et al. Long noncoding RNA HULC modulates the phosphorylation of YB-1 through serving as a scaffold of extracellular signal-regulated kinase and YB-1 to enhance hepatocarcinogenesis. Hepatology 2017;65:1612–27.
15. Karreth FA, Reschke M, Ruocco A, Ng C, Chapuy B, Leopold V, et al. The BRAF pseudogene functions as a competitive endogenous RNA and induces lymphoma in vivo. Cell 2015;161:319–32.
16. Yang F, Zhang L, Huo XS, Yuan JH, Xu D, Yuan SX, et al. Long noncoding RNA high expression in hepatocellular carcinoma facilitates tumor growth through enhancer of zeste homolog 2 in humans. Hepatology 2011;54:1679–89.
17. Yuan JH, Yang F, Wang F, Ma JZ, Guo YJ, Tao QF, et al. A long noncoding RNA activated by TGF-beta promotes the invasion-metastasis cascade in hepatocellular carcinoma. Cancer Cell 2014;25:666–81.
18. Quagliata L, Matter MS, Piscuoglio S, Arabi L, Ruiz C, Procino A, et al. Long noncoding RNA HOTTIP/HOXA13 expression is associated with disease progression and predicts outcome in hepatocellular carcinoma patients. Hepatology 2014;59:911–23.
19. Yan XL, Fu CJ, Chen L, Qin JH, Zeng Q, Yuan HF, et al. Mesenchymal stem cells from primary breast cancer tissue promote cancer proliferation and enhance mammosphere formation partially via EGF/EGFR/Akt pathway. Breast Cancer Res Treat 2012;132:153–64.
20. Waghray M, Yalamanchili M, Dziubinski M, Zeinali M, Erkkinen M, Yang H, et al. GM-CSF mediates mesenchymal-epithelial cross-talk in pancreatic cancer. Cancer Discov 2016;6:886–99.
21. Zhou JN, Zeng Q, Wang HY, Zhang B, Li ST, Nan X, et al. MicroRNA-125b attenuates epithelial-mesenchymal transitions and targets stem-like liver cancer cells through small mothers against decapentaplegic 2 and 4. Hepatology 2015;62:801–15.
22. Mani SA, Guo W, Liao MJ, Eaton EN, Ayyanan A, Zhou AY, et al. The epithelial-mesenchymal transition generates cells with properties of stem cells. Cell 2008;133:704–15.
23. Cancer Genome Atlas Research Network, Weinstein JN, Collisson EA, Mills GB, Shaw KR, Ozenberger BA, et al. The Cancer Genome Atlas Pan-Cancer analysis project. Nat Genet 2013;45:1113–20.
24. Yuan J, Yue H, Zhang M, Luo J, Liu L, Wu W, et al. Transcriptional profiling analysis and functional prediction of long noncoding RNAs in cancer. Oncotarget 2016;7:8131–42.
25. Gupta RA, Shah N, Wang KC, Kim J, Horlings HM, Wong DJ, et al. Long non-coding RNA HOTAIR reprograms chromatin state to promote cancer metastasis. Nature 2010;464:1071–6.
26. Fang D, Hawke D, Zheng Y, Xia Y, Meisenhelder J, Nika H, et al. Phosphorylation of beta-catenin by AKT promotes beta-catenin transcriptional activity. J Biol Chem 2007;282:11221–9.
27. Ha NC, Tonozuka T, Stamos JL, Choi HJ, Weis WI. Mechanism of phosphorylation-dependent binding of APC to beta-catenin and its role in beta-catenin degradation. Mol Cell 2004;15:511–21.
28. Wang Y, Xu Z, Jiang J, Xu C, Kang J, Xiao L, et al. Endogenous miRNA sponge lincRNA-RoR regulates Oct4, Nanog, and Sox2 in human embryonic stem cell self-renewal. Dev Cell 2013;25:69–80.
29. Salmena L, Poliseno L, Tay Y, Kats L, Pandolfi PP. A ceRNA hypothesis: the Rosetta Stone of a hidden RNA language? Cell 2011;146:353–8.
30. Rucki AA, Foley K, Zhang P, Xiao Q, Kleponis J, Wu AA, et al. Heterogeneous stromal signaling within the tumor microenvironment controls the metastasis of pancreatic cancer. Cancer Res 2017;77:41–52.
31. Zhao L, Ji G, Le X, Wang C, Xu L, Feng M, et al. Long noncoding RNA LINC00092 acts in cancer-associated fibroblasts to drive glycolysis and progression of ovarian cancer. Cancer Res 2017;77:1369–82.
32. Borriello L, Nakata R, Sheard MA, Fernandez GE, Sposto R, Malvar J, et al. Cancer-associated fibroblasts share characteristics and protumorigenic activity with mesenchymal stromal cells. Cancer Res 2017;77:5142–5157.
33. Yang X, Lin Y, Shi Y, Li B, Liu W, Yin W, et al. FAP promotes immunosuppression by cancer-associated fibroblasts in the tumor microenvironment via STAT3-CCL2 signaling. Cancer Res 2016;76:4124–35.
34. Korkaya H, Liu S, Wicha MS. Breast cancer stem cells, cytokine networks, and the tumor microenvironment. J Clin Invest 2011;121:3804–9.
35. Freese KE, Kokai L, Edwards RP, Philips BJ, Sheikh MA, Kelley J, et al. Adipose-derived stems cells and their role in human cancer development, growth, progression, and metastasis: a systematic review. Cancer Res 2015;75:1161–8.
36. McLean K, Gong Y, Choi Y, Deng N, Yang K, Bai S, et al. Human ovarian carcinoma-associated mesenchymal stem cells regulate cancer stem cells and tumorigenesis via altered BMP production. J Clin Invest 2011;121:3206–19.
37. Malakar P, Shilo A, Mogilevsky A, Stein I, Pikarsky E, Nevo Y, et al. Long noncoding RNA MALAT1 promotes hepatocellular carcinoma development by SRSF1 upregulation and mTOR activation. Cancer Res 2017;77:1155–67.
38. Wang Y, He L, Du Y, Zhu P, Huang G, Luo J, et al. The long noncoding RNA lncTCF7 promotes self-renewal of human liver cancer stem cells through activation of Wnt signaling. Cell Stem Cell 2015;16:413–25.
39. Yuan SX, Yang F, Yang Y, Tao QF, Zhang J, Huang G, et al. Long noncoding RNA associated with microvascular invasion in hepatocellular carcinoma promotes angiogenesis and serves as a predictor for hepatocellular carcinoma patients' poor recurrence-free survival after hepatectomy. Hepatology 2012;56:2231–41.
40. Ye X, Tam WL, Shibue T, Kaygusuz Y, Reinhardt F, Ng Eaton E, et al. Distinct EMT programs control normal mammary stem cells and tumour-initiating cells. Nature 2015;525:256–60.
41. Essien BE, Sundaresan S, Ocadiz-Ruiz R, Chavis A, Tsao AC, Tessier AJ, et al. Transcription factor ZBP-89 drives a feedforward loop of beta-catenin expression in colorectal cancer. Cancer Res 2016;76:6877–87.
42. Dominguez-Brauer C, Khatun R, Elia AJ, Thu KL, Ramachandran P, Baniasadi SP, et al. E3 ubiquitin ligase Mule targets beta-catenin under conditions of hyperactive Wnt signaling. Proc Natl Acad Sci U S A 2017;114:E1148–E57.
43. Chai S, Ng KY, Tong M, Lau EY, Lee TK, Chan KW, et al. Octamer 4/microRNA-1246 signaling axis drives Wnt/beta-catenin activation in liver cancer stem cells. Hepatology 2016;64:2062–76.
44. Ding Q, Xia W, Liu JC, Yang JY, Lee DF, Xia J, et al. Erk associates with and primes GSK-3beta for its inactivation resulting in upregulation of beta-catenin. Mol Cell 2005;19:159–70.
45. Clevers H. Wnt/beta-catenin signaling in development and disease. Cell 2006;127:469–80.
46. Cesana M, Cacchiarelli D, Legnini I, Santini T, Sthandier O, Chinappi M, et al. A long noncoding RNA controls muscle differentiation by functioning as a competing endogenous RNA. Cell 2011;147:358–69.
47. Qu L, Ding J, Chen C, Wu ZJ, Liu B, Gao Y, et al. Exosome-transmitted lncARSR promotes sunitinib resistance in renal cancer by acting as a competing endogenous RNA. Cancer Cell 2016;29:653–68.